Electrically Insulating Thermal Nano-Oils Using 2D Fillers

Jaime Taha-Tijerina,[†,‡,∥] Tharangattu N. Narayanan,[†,∥] Guanhui Gao,[†,§] Matthew Rohde,[†] Dmitri A. Tsentalovich,[⊥] Matteo Pasquali,[⊥] and Pulickel M. Ajayan[†,⊥,*]

[†]Department of Mechanical Engineering and Materials Science, Rice University, Houston, Texas 77005, United States, [‡]Prolec GE Internacional, S. de R.L. de C.V., Monterrey, NL, México, [§]College of Chemistry and Chemical Engineering, Ocean University of China, Qingdao, China, and [⊥]Department of Chemical and Biomolecular Engineering, Rice University, Houston, Texas 77005, United States. [∥]These authors contributed equally to this work.

ABSTRACT

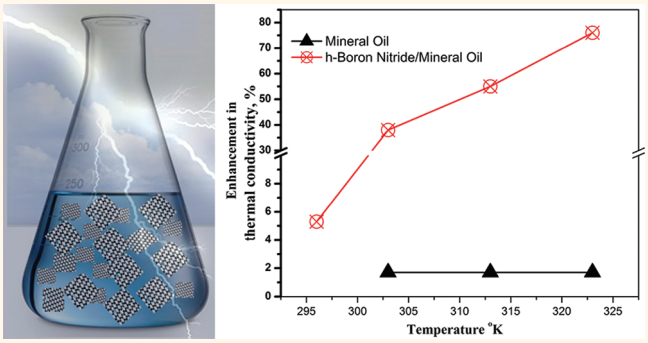

Different nanoscale fillers have been used to create composite fluids for applications such as thermal management. The ever increasing thermal loads in applications now require advanced operational fluids, for example, high thermal conductivity dielectric oils in transformers. These oils require excellent filler dispersion, high thermal conduction, but also electrical insulation. Such thermal oils that conform to this thermal/electrical requirement, and yet remain in highly suspended stable state, have not yet been synthesized. We report here the synthesis and characterization of stable high thermal conductivity Newtonian nanofluids using exfoliated layers of hexagonal boron nitride in oil without compromising its electrically insulating property. Two-dimensional nanosheets of hexagonal boron nitride are liquid exfoliated in isopropyl alcohol and redispersed in mineral oil, used as standard transformer oil, forming stable nanosuspensions with high shelf life. A high electrical resistivity, even higher than that of the base oil, is maintained for the nano-oil containing small weight fraction of the filler (0.01 wt %), whereas the thermal conductivity was enhanced. The low dissipation factor and high pour point for this nano-oil suggests several applications in thermal management.

KEYWORDS: thermal management · nanofluids · 2D materials · h-BN · electrically insulating fluids

Nanofluid-based heat transfer plays an important role in diverse fields such as microelectronics, high voltage power transmission systems, automobiles, solar cells, biopharmaceuticals, medical therapy/diagnosis, and nuclear cooling.[1−5] The miniaturization and high efficiency of electrical/electronic devices in these fields demand successful heat management and energy-efficient fluid-based heat-transfer systems. High thermal conductivity is essential for such heat-transfer fluids. Conventional heat-transfer fluids such as water, ethylene glycol, and engine/transformer oils are typically low-efficiency heat-transfer fluids.[2−5] Solid materials have higher thermal conductivity than these conventional fluids, and the advent of "nanofluids" for heat transfer, where solid ultrafine particles such as oxide, nitride, and carbide ceramics, metals, semiconductors, carbon nanotubes, and composite materials are suspended in fluids, has provided better thermal conductivities.[5−8] Recent advances in layered materials enable large-scale synthesis of various two-dimensional (2D) materials.[9] Two-dimensional materials can be good choices as nanofillers in heat-transfer fluids, due to the high surface area they have available for heat transfer. Among various 2D materials, hexagonal boron nitride or graphene exhibits versatile properties such as superb thermal conductivity, excellent mechanical stability, and remarkable chemical inertness.[10] As an insulating material with very high thermal conductivity, hexagonal boron nitride surpasses other nanofillers and is an attractive material for high thermal conductivity and electrically insulating composites.[11,12] However, theoretical studies indicate that high thermal conductivities can only be achieved from the (002) planes of hexagonal boron nitride;[13] exfoliated hexagonal boron nitride (h-BN) can give maximum exposure to these (002) lattice planes.

Heat transfer using fluids is a complex phenomenon, and various factors such as fluid stability, composition, viscosity, surface charge, interface, and morphology of the dispersed particles influence the observed results.[2,14−17] The reported high thermal conductivity values of nanofluids are far from satisfactory for practical implementations.[3] The improvement in thermal conductivity cannot be achieved by

* Address correspondence to ajayan@rice.edu.

Received for review October 7, 2011 and accepted January 24, 2012.

Published online January 24, 2012
10.1021/nn203862p

increasing the solid filler amount beyond a limit because increase in filler concentration will increase the viscosity which will adversely affect the fluid properties. Hence, the search for new nanofillers which can get high thermal conductivities at lower filler fractions is important.[18] Moreover, fillers that would provide increased thermal conductivities but do not increase electrical conductivity are mostly ceramic particles, and conventional ceramic particles often have dispersion or settling problems and are not well-dispersible. Here we report the synthesis and characterization of a novel nanofluid containing h-BN in mineral oil (MO; standard electrical transformer oil, Nytro 10XN). The properties of these fluids are also compared with its 2D carbon analogue, graphene (exfoliated graphite). Graphene fluids represent both thermally and electrically conducting fluids, finding applications like thermal management coupled with static charge dissipation in oil tanks, while h-BN fluids represent thermally conducting and electrically insulating fluids.

RESULTS AND DISCUSSION

The schematic of liquid exfoliation of micrometer-sized layered h-BN crystals to 2D h-BN nanosheets is depicted in Figure 1a. The TEM of the exfoliated h-BN is shown in Figure 1b. The h-BN powder is exfoliated into thin layers containing few atomic layers, ~5−10 layers (more TEM and HR-TEM images for further evidence are provided in Supporting Information, Figure S1). The corresponding selected area electron diffraction is shown in the inset of Figure 1b. The diffraction rings show the crystallinity of the h-BN layers with rotational disorder.[19] The TEM and HRTEM images of exfoliated graphite (graphene, G sheets) are provided in the Supporting Information (Figure S2). The HR-TEM indicates that G typically contains ~8−10 atomic layers. The X-ray diffraction (XRD, using Rigaku Cu Kα) pattern of h-BN (that of graphene is provided in the Supporting Information, Figure S3) is depicted in Figure 1c. The XRD of dried h-BN nanosheet powders shows a prominent (002) peak indicating a maximum exposure of 002. Raman spectrum of h-BN at 1369 cm^{-1} originates from E_{2g} mode of B−N bond vibration as seen in Figure 1d. The Raman spectrum of graphene shows the disorder-induced D peak at ~1350 cm^{-1}, G peak at ~1595 cm^{-1}, and 2D peak at 2695 cm^{-1} (please see Supporting Information).[19] The photographs of various nanofluids are shown in Figure 2 (photograph in a dark background is provided in the Supporting Information, Figure S4, showing the transparency of h-BN/MO in two different concentrations). Figure 3 discusses the thermal and electrical properties of various nanofluids in different filler fractions. Figure 4a depicts the correlation of experimental and theoretical viscosity values of nanofluids, and Figure 4b is the experimental pour point values of MO, h-BN/MO, and graphene/MO.

The nanofluid with low filler fractions of h-BN (0.01−0.1 wt %) is highly stable in MO with a high shelf life (found to be stable even after 3 months) without any surfactant. The zeta-potential (measured using Malvern Zen 3600 Zetasizer (Zetasizer Nano)) of the 0.1 wt % h-BN/MO nanofluid is found to be ~22 mV, indicating the stability of the nanofluid; later in this paper, we have substantiated the stability of the fluid using viscosity measurements. However, the graphene nanofluid is relatively less stable with a relatively low zeta-potential value of ~10 mV. The exfoliated layers can be stabilized in MO *via* molecular interactions as well as Brownian motion. The interaction of oleophilic layers (particularly that of h-BN) with the MO can contribute to the enhanced stability of the suspensions (the high hydrodynamic radius of ~1000 nm found from dynamic light scattering studies (DLS) of h-BN/MO and graphene/MO (~1300 nm) also suggests interaction between layers due to their oleophilic nature). The possible interaction between exfoliated layers and MO is further studied *via* viscosity measurements, theoretical modeling, and pour point evaluation.

Figure 3a shows the temperature-dependent thermal conductivities of both h-BN/MO and graphene/MO fluids at various weight percentages of the fillers. The thermal conductivity of MO (at room temperature, thermal conductivity is ~0.115 W/mK, agreeing well with standard values reported) did not show any temperature dependence, as reported by others.[20] However, the nanofluids show a temperature-dependent variation in the thermal conductivity, indicating the role of nanoparticles in thermal conductivity.[14] Effective thermal conductivities (k_{eff}) of nanofluids increases with temperature (measurements are done from room temperature to 50 °C), indicating the role of Brownian motion on thermal conductivities measured, in accordance with Maxwell predictions.[5,16] Other factors influencing the k_{eff} of nanofluids is the liquid layering and viscosity. The oleophilic nature h-BN allows for good interfacial interaction (layering) with MO as is inferred from the enhanced hydrodynamic radius from DLS studies. The liquid layering at the particle−liquid interface is predicted as the most important mechanism for effective thermal conductivity enhancement in nanofluids by many researchers.[5,16] The viscosity of the nanofluids decreases significantly with temperature (from 16 mm^2/s at room temperature to 2.2 mm^2/s at 100 °C) (Figure 4a), while the enhancement in viscosity with the addition of nanofillers is very small. This is an added advantage of the low filler fractions since the increase in viscosity will decrease the effective thermal conductivity values as well as flow characteristics of the fluid. These nanofluids are stabilized in the carrier fluid (MO) without any surfactant. The surfactants can decrease the thermal conductivity of the nanofluids since surfactants introduce defects at the interfaces.[21] The free phonon/electron movement is affected by these defects, and hence a surfactant-free stable suspension can provide much better thermal conductivity.

Figure 3a shows the enhancement in thermal conductivity with the increase in weight fraction of h-BN or

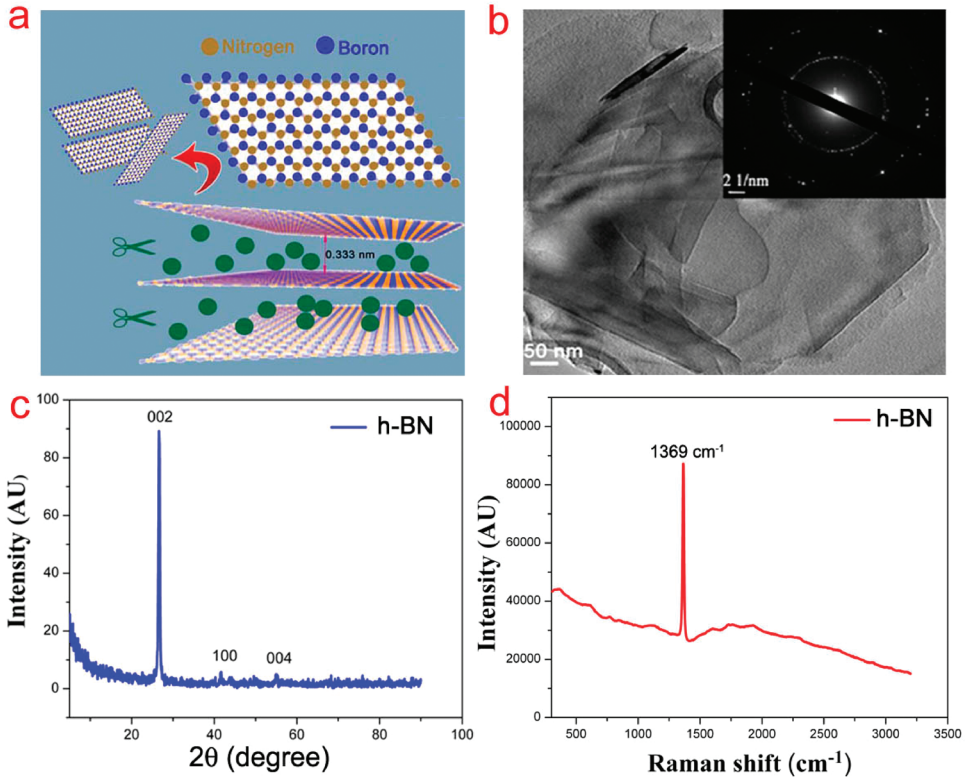

Figure 1. (a) Schematic of liquid exfoliation of h-BN crystals in to 2D h-BN nanosheets using sonication and centrifugation. IPA (green spheres in figure) is used for liquid exfoliation. (b) TEM image of h-BN (corresponding SAED pattern is shown in inset) showing few layered sheets. SAED pattern shows the crystallinity of the exfoliated nanosheets with adjacent nanosheets having rotational disorder. (c) XRD pattern of dried h-BN nanosheet powders, and (d) micro-Raman spectrum (633 nm excitation) of h-BN nanosheets depicting the E_{2g} mode of B−N vibrations in h-BN nanosheets.

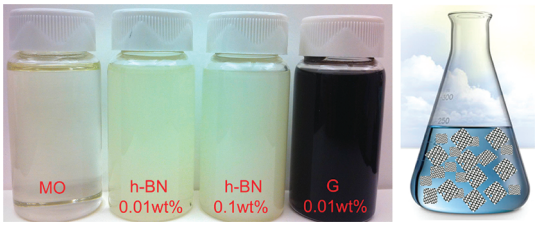

Figure 2. (Left) Photographs of pure MO and various suspensions of h-BN/MO and graphene/MO in a white background. (Right) Schematic of 2D layers (h-BN/graphene) in MO stabilized *via* Brownian motion and interactions with MO.

graphene and increase in temperature of measurements. The 0.1 wt % h-BN/MO shows an enhanced thermal conductivity $((k_{eff}/k_0) - 1)\%$ of ~76%. The morphology of nanofillers can strongly influence the thermal conductivity of the nanofluid. The volume fractions and conductivities of two phases will determine the upper (where the nanofillers will form continuous phase) and lower (carrier fluid serves as the continuous phase) boundary values of the effective thermal conductivity of the nanofluid. A theoretical model of the effective thermal conductivity of the h-BN/MO nanofluid is performed using a classical effective medium theory known as Hashin−Shtrikman (H−S) theory.[18] In both cases, for h-BN/MO or graphene/MO, the ratio of k_p/k_f is >1, where k_p is the thermal conductivity of h-BN or graphene and k_f is the thermal conductivity of MO. The lower boundary value (since the nanofillers fraction, φ, is very low, 0.01 wt %) for effective thermal conductivity of h-BN/MO, k_e is calculated using the following equation:

$$\frac{k_e}{k_f} = 1 + \frac{3\varphi\left(\frac{k_p}{k_f} - 1\right)}{\frac{k_p}{k_f} + 2 - \varphi\left(\frac{k_p}{k_f} - 1\right)} \quad (1)$$

The calculated value 0.1184 W/mK matches well with the lowest experimental value obtained for 0.01 wt % h-BN/MO nanofluid (0.119W/mK). Keblinski *et al.* demonstrated that clustering of the nanofillers can increase the thermal conductivity of nanofluids. The clustering effect is relatively higher in graphene/MO, and hence, it is relatively less stable than h-BN/MO. This is also inferred from dynamic light scattering studies (size ~ 1300 nm) and HRTEM studies (Supporting Information). This can be the reason for slightly higher thermal conductivity values for graphene/MO than for h-BN/MO (for more details, see Supporting Information, Figure S5) (~1% enhancement in effective thermal conductivity for graphene/MO compared to h-BN/MO), although graphite and h-BN have the same bulk thermal conductivity values. Moreover, the percentage of enhancement in thermal conductivity obtained for 0.01 wt % graphene/MO nanofluid is in

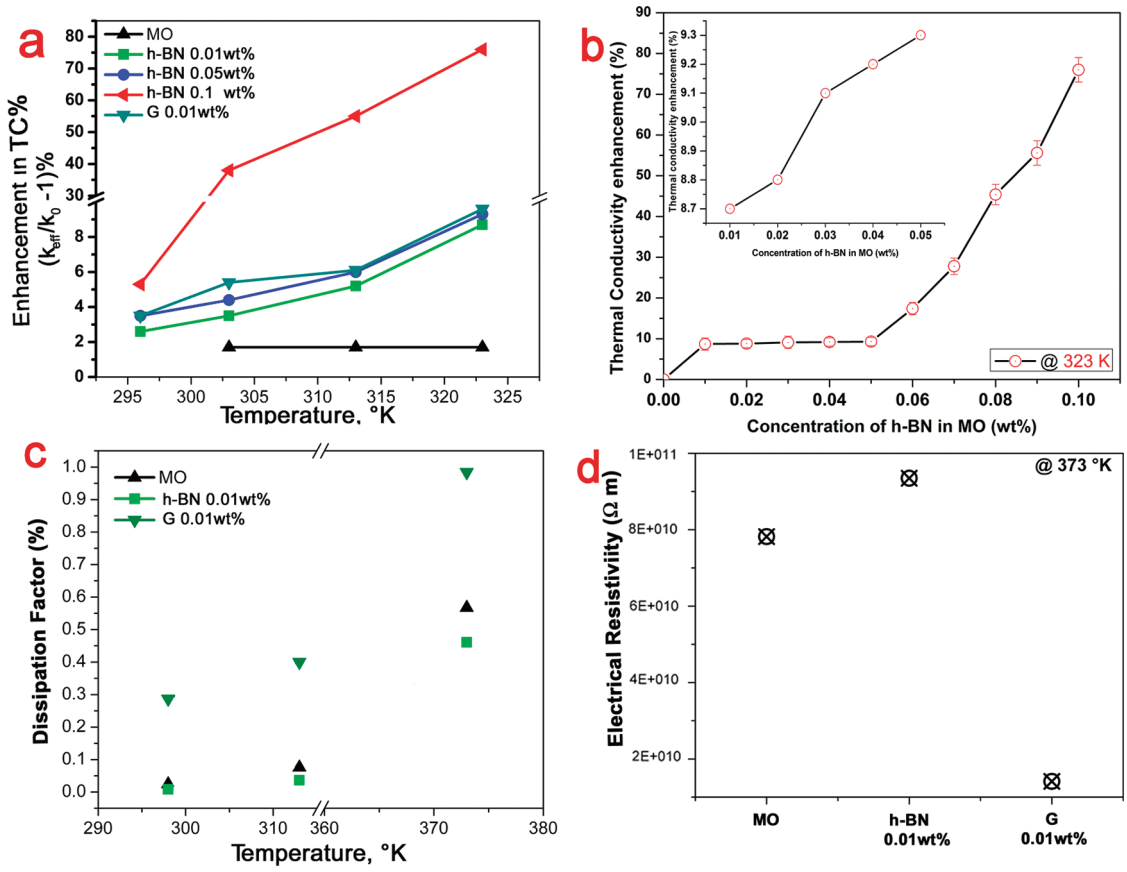

Figure 3. (a) Temperature-dependent effective thermal conductivity (TC) enhancement of various nanofluids (percentage of filler amount is mentioned). Pure MO shows no variation in TC with temperature. All nanofluids show an enhancement in thermal conductivity with temperature, indicating the contribution of Brownian motion in thermal conductivity enhancement. (b) Enhancement in thermal conductivity with increase in the h-BN concentration in MO measured at 323 K. This indicates the formation of percolation channels for thermal conduction by high surface area h-BN flakes, as explained by network model (inset shows the variation in TC between 0.01 and 0.05 wt %). The error bars attached to the results incorporate the variation in the different measurements. (c) Temperature-dependent dissipation factor variation of various nanofluids. h-BN/MO shows the lowest DF, indicating their enhanced dielectric nature, and (d) electrical resistivity variation of nanofluids. h-BN/MO shows the highest electrical resistivity, while graphene/MO shows the lowest electrical resistance in comparison to pure MO.

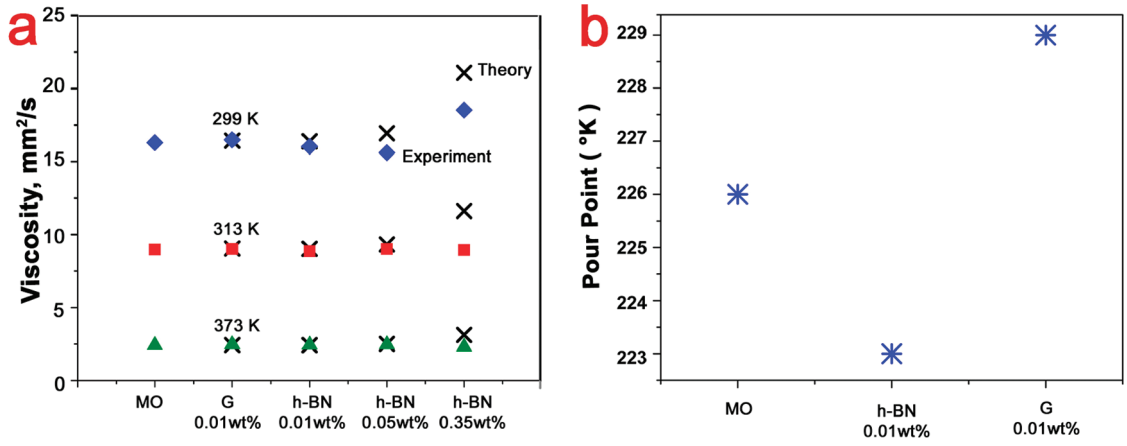

Figure 4. (a) Temperature-dependent viscosity variation of nanofluids (black crosses (X) indicate theoretical values calculated using the theory of Hinch and Leal, and colored points indicate the experimental values). Small deviations from the theoretical values of viscosity at higher concentrations of h-BN/MO may be a result of a transition from a dilute to a semidilute phase or due to the onset of some small aggregation between the h-BN nanosheets. (b) Pour point variation of various fluids. The lowering of the pour point of h-BN/MO indicates the possible molecular interactions between h-BN and MO.

agreement with that of recently reported values for graphene-based nanofluids.[22,23] Figure 3b shows the variation in measured thermal conductivity at 323 K for different h-BN/MO fluids with varying h-BN concentration.

The thermal conductivity of h-BN/MO fluids is found to be gradually increased with h-BN filler concentration, from 0.01 to 0.1 wt %. This high thermal conductivity value even at smaller filler concentrations is due to the high surface area of h-BN sheets. The increase in thermal conductivity with filler fractions indicates that at higher concentrations it is not following Maxwell's classical theory where it will not vary much with concentration, while they follow a network model like graphene fluids. This indicates the contribution of percolation mechanism for thermal conductivity. Moreover, like graphene fluids but unlike graphene oxide[24] or CNT fluids,[22] the thermal conductivity of h-BN/MO fluids found to increase with temperature (Figure 3a). However, the temperature-dependent variations in thermal conductivity indicate that it is not just the percolation mechanism that increases the thermal conductivity, as explained in the network model, but Brownian motion also contributes to the thermal conductivity of h-BN and graphene 2D material-based nanofluids. The thermal conductivity measurements above 50 °C are also carried out. The percentage of enhancement in thermal conductivity for 0.1 wt % h-BN/MO nanofluid at 373 K ranges from 80 to 100% in different measurements. The wide range in thermal conductivity values obtained at higher temperatures (>50 °C for oil based nanofluids) is due to the enhanced free convection at higher temperatures. Hence, even though it is obvious that the thermal conductivity of the h-BN/MO nanofluid is enhanced at high temperatures (>50 °C), the accurate percentage of enhancement is hard to measure.

The use of nanofluids for thermal management in electrical devices, such as transformers, also necessitates the study of their electrical properties. The dissipation factor (DF) or liquid power factor, which is a measure of the dielectric loss in the system under the presence of an alternating electric field, is measured (liquid power factor using ASTMD-924 and % DF using ASTMD-1169; measurements have been done at 2000 V and 60 Hz; the values matches in both cases) for various nanofluids and is plotted in Figure 3c. h-BN/MO exhibits the lowest DF, while graphene/MO exhibits an enhanced value compared to MO at all measured temperatures. Since DF represents the ratio of equivalent series resistance (ESR) to capacitive reactance, the decrease in DF indicates the decrease in dielectric losses in the material. The electrical resistivity (ASTM D1169) of the nanofluids is also found to be affected by various nanofillers (Figure 3d). The h-BN/MO exhibited higher resistivity (9.35E10 Ωm), while graphene/MO showed lower resistivity (1.41E10 Ωm) compared to MO (7.82E10 Ωm). This is understandable as h-BN is electrically insulating, while graphene is electrically conducting. These studies are important for the development of nanofluids for thermal and electrical management. The comparison of our obtained results for h-BN/MO with the existing literature (various nanofillers with different morphology) indicates that this is a leap in the development of highly thermally conducting nanofluids with lower filler fractions but without losing the electrically insulating properties of the base fluid. A detailed survey on the development of oil-based nanofluids for thermal management is shown in Table 1 in the Supporting Information.

To further understand the stability of the nanofluid, shear viscosity studies were conducted with a TA Instruments ARES rheometer (Figure 4a). Temperature-dependent shear viscosity measurements for different concentrations of h-BN/MO (viscosity measurements of 0.01 wt % graphene/MO also shown for comparison) are shown in Figure 4a. MO behaves like a Newtonian fluid since its viscosity is independent of shear rate, and the viscosity of MO decreases with increasing temperature. Addition of h-BN up to 0.05 wt % to MO does not measurably alter its viscosity for the entire range of temperatures tested. At 298 K (25 °C) and 0.35 wt % of h-BN, the viscosity increases, but the behavior of the fluid is still Newtonian. Newtonian behavior in solutions of nanoparticles indicates that the interactions between the particles are very weak.[25] This suggests that the h-BN/MO nanofluids are relatively stable colloidal systems. Moreover, the relatively small increase in viscosity (<30%) at 0.35 wt % is evidence that the solution is not flocculating.[26] This enhancement in viscosity is consistent with the theoretical predictions of Hinch and Leal for dilute solutions of noninteracting oblate spheroids (considering the layered morphology of h-BN and graphene), for which the viscosity is described by the following equation.[27]

$$\eta = \left(\frac{32}{15\pi}\right)\left(\frac{\phi\eta_s}{p}\right) + \eta_s \qquad (2)$$

where φ is the volume fraction of nanoparticles in solution, η_s is the solvent viscosity, and p is the dimensional ratio (the shortest nanoparticle dimension to the largest one). In order to calculate p, the largest dimension of the nanoparticles was measured with dynamic light scattering. Assuming the h-BN and graphene have a thickness of around 4 nm (few-layered graphene and h-BN, inferred from the HRTEM images), the corresponding p values are 0.008 for h-BN and 0.006 for graphene. The theory agrees well with the experimental rheological data (Figure 4a), suggesting that the average number of layers of h-BN and graphene in MO is around 10. The pour point, which is the lowest temperature at which the fluid can flow (pumpable temperature), seems to be affected by the nanofillers of h-BN and graphene (Figure 4b), showing that it is not just a colligative property but also depends on the nature of nanofillers (for h-BN/MO, pour point is lowered, and for graphene/MO, pour point is enhanced) and intermolecular interactions. The lowering of the pour point can be attributed to the nanoscale dimensions of the fillers (here h-BN) and high intermolecular interactions and liquid layering (MO) with the h-BN.[28] The h-BN could substantially increase the thermal conductivity of MO

while lowering the pour point of MO, which are both desirable properties of heat-transfer fluids. Small deviations from the theoretical values of viscosity at higher concentrations of h-BN may be a result of a transition from a dilute to a semidilute phase or due to the onset of some small aggregation between the h-BN nanosheets.

CONCLUSION

We have demonstrated here a stable Newtonian nanofluid with 2D fillers of h-BN in a mineral oil, normally used in transformers, having high thermal conductivity. The h-BN/MO nanofluid is also an electrically insulating fluid and has a lower freezing point than the pure MO. The h-BN/MO results are compared with graphene/MO, which appears to be more electrically conductive though it is also highly thermally conductive. Our electrical and thermal analysis of these unique h-BN/MO fluids shows that these may possibly be the next generation thermal nano-oils for lubrication, capable of efficient thermal management in heavy duty machinery such as transformers.

METHODS

Synthesis of h-BN/MO and Graphene/MO Nanofluids. Both the nanofluids were synthesized by the liquid exfoliation method. The micrometer-sized h-BN powder purchased from Sigma Aldrich (1 μm, 98%) is extensively sonicated (3 h) in isopropyl alcohol (IPA, room temperature surface tension $\sim$ 23 mN/m), keeping the temperature (300 K) of the sonicator water bath constant. After sonication, the solution is centrifuged for 30 min with a high rate of 1500 rpm. The whitish supernatant is collected and is vacuum-filtered. The collected white powder is redispersed in MO by sonication at room temperature.

The graphene (G) is prepared by the same liquid exfoliation method using graphitic powder (Bay Carbon, Inc. SP-1 grade 325 mesh). Dimethyl formamide is used as the exfoliation medium (room temperature surface tension $\sim$ 37 mN/m). The initial powder is sonicated for 3 h, and the resultant solution is centrifuged at a high rate of 3000 rpm. The resultant blackish supernatant is collected and filtered, and the powder is redispersed in MO by sonication at room temperature. Surfactants are not used in both cases.

Thermal Conductivity Measurement Setup and Precautions. Thermal conductivity measurements on h-BN and graphene nanofluids of different weight percentages were carried out using a KD2 probe (Decagon Device Inc., model KD2 Pro). This device is based on the transient hot-wire (a fast and accurate method for fluid thermal conductivity measurements), where a finite length wire is completely immersed in a finite fluid medium and the wire is electrically heated. While the wire is heating up, the change in resistance (thus its temperature) is measured as a function of time using a Wheatstone bridge circuitry. The thermal conductivity (TC) value is determined from the heating power and the slope of the temperature change with logarithmic time scale. The instrument uses a 1.3 mm diameter by 60 mm long stainless steel probe (KS-1 probe) that is completely immersed in the nanofluid to obtain the effective thermal conductivity (k_f) of nanofluids. This probe has been calibrated using a standard fluid, glycerol, and the conductivity value is verified up to 3 decimal points. Temperature-dependent measurements were done using a thermal bath, and samples were thermally equilibrated before each measurement. The measured values are compared with the base fluid (MO) thermal conductivity (k_0). The possible errors due to the free and forced convection mechanisms have been minimized by aligning the sensor orientation in the vertical direction with the fluid sample container (error due to free convection, $\delta g \propto 1/d$, where d is the characteristic dimension of sensor and d is higher in the vertical orientation of the sensor (the role of alignment of sensor probe in the measurement is discussed in Supporting Information, Figure S6) and vibration isolation of the measurements, and moreover, the higher viscosity of MO than water also minimizes the error due to free convection. Thermal conduction happens through direct molecular interactions and there is no bulk fluid flow. However, convection heat transfer occurs when there is bulk fluid flow. Hence, during measurements, it is necessary to isolate all kinds of convection mechanisms that can contribute error to the thermal conductivity measurement.

Conflict of Interest: The authors declare no competing financial interest.

Acknowledgment. J.T.-T. acknowledges the support from Prolec GE Internacional, S. de R.L. de C.V., Monterrey, Mexico, and CONACYT (213780). P.A., T.N., and J.T.-T. acknowledge funding from the Army Research Office through MURI program on novel free-Standing 2D crystalline materials focusing on atomic layers of nitrides, oxides, and sulfides. Authors greatly acknowledge Dr. Bhabendra Pradhan, from NanoHoldings, for fruitful discussions. P.A. acknowledges funding from the MURI program on graphene supported by the Office of Naval Research. M. P. acknowledges funding from AFOSR grant FA9550-09-1-0590 and from the Welch Foundation grant C-1668.

Supporting Information Available: Details of graphene (XRD, Raman), additional TEM pictures for exfoliated h-BN and graphene, a table citing detailed achievements so far attained in thermal/electrical management fluids, and details of the thermal conductivity measurements. This material is available free of charge *via* the Internet at http://pubs.acs.org.

REFERENCES AND NOTES

1. Balandin, A. A. Thermal Properties of Graphene and Nanostructured Carbon Materials. *Nat. Mater.* **2011**, *10*, 569–581.
2. Gao, J. W.; Zheng, R. T.; Ohtani, H.; Zhu, D. S.; Chen, G. Experimental Investigation of Heat Conduction Mechanisms in Nanofluids. Clue on Clustering. *Nano Lett.* **2009**, *9*, 4128–4132.
3. Zhi, C.; Xu, Y.; Bando, Y.; Golberg, D. Highly Thermoconductive Fluid with Boron Nitride Nanofillers. *ACS Nano* **2011**, *5*, 6571–6577.
4. Botha, S. S.; Ndungu, P.; Bladergroen, B. J. Physicochemical Properties of Oil-Based Nanofluids Containing Hybrid Structures of Silver Nanoparticles Supported on Silica. *Ind. Eng. Chem. Res.* **2011**, *50*, 3071–3077.
5. Baby, T. T.; Sundara, R. Synthesis and Transport Properties of Metal Oxide Decorated Graphene Dispersed Nanofluids. *J. Phys. Chem. C* **2011**, *115*, 8527–8533.
6. Eastman, J. A.; Choi, S. U. S.; Li, S.; Yu, W.; Thompson, L. J. Anomalously Increased Effective Thermal Conductivities of Ethylene Glycol-Based Nanofluids Containing Copper Nanoparticles. *Appl. Phys. Lett.* **2001**, *78*, 718–720.
7. Choi, C.; Yoo, H. S.; Oh, J. M. Preparation and Heat Transfer Properties of Nanoparticle-in-Transformer Oil Dispersions as Advanced Energy-Efficient Coolants. *Curr. Appl. Phys.* **2008**, *8*, 710–712.
8. Xie, H.; Chen, L. Review on the Preparation and Thermal Performances of Carbon Nanotube Contained Nanofluids. *J. Chem. Eng. Data* **2011**, *56*, 1030–1041.
9. Colleman, J. N.; Lotya, M.; O'Neill, A.; Bergin, S. D.; King, P. J.; Khan, U.; Young, K.; Gaucher, A.; De, S.; Smith, R. J.; *et al.* Two-Dimensional Nanosheets Produced by Liquid Exfoliation of Layered Materials. *Science* **2011**, *331*, 568–571.

10. Pakdel, A.; Zhi, C.; Bando, Y.; Nakayama, T.; Golberg, D. Boron Nitride Nanosheet Coatings with Controllable Water Repellency. *ACS Nano* **2011**, *5*, 6507–6515.
11. Zhi, C.; Bando, Y.; Tang, C.; Golberg, D. Boron Nitride Nanotubes. *Mater. Sci. Eng. Res.* **2010**, *70*, 92–111.
12. Yu, J.; Qin, L.; Hao, Y.; Kuang, S.; Bai, X.; Chong, Y.; Zhang, W.; Wang, E. Vertically Aligned Boron Nitride Nanosheets: Chemical Vapor Synthesis, Ultraviolet Light Emission, and Superhydrophobicity. *ACS Nano* **2010**, *4*, 414–422.
13. Zhi, C. Y.; Bando, Y.; Terao, T.; Tang, C.; Kuwahara, H.; Golberg, D. Towards Highly Thermo-Conductive Electrically Insulating Polymeric Composites with Boron Nitride Nanotubes as Fillers. *Adv. Funct. Mater.* **2009**, *19*, 1857–1862.
14. Aravind, S. S. J.; Baskar, P.; Baby, T. T.; Sabareesh, R. K.; Das, S.; Ramaprabhu, S. Investigation of Structural Stability, Dispersion, Viscosity, and Conductive Heat Transfer Properties of Functionalized Carbon Nanotube Based Nanofluids. *J. Phys. Chem. C* **2011**, *115*, 16737–16744.
15. Krishnamurthy, S.; Bhattacharya, P.; Phelan, P. E.; Prasher, R. S. Enhanced Mass Transport in Nanofluids. *Nano Lett.* **2006**, *6*, 419–423.
16. Shima, P. D.; Philip, J.; Raj, B. Synthesis of Aqueous and Nonaqueous Iron Oxide Nanofluids and Study of Temperature Dependence on Thermal Conductivity and Viscosity. *J. Phys. Chem. C* **2010**, *114*, 18825–18833.
17. Keblinski, P.; Phillpot, S. R.; Choi, S. U. S.; Eastman, J. A. Mechanisms of Heat Flow in Suspensions of Nano-Sized Particles. *Int. J. Heat Mass Transfer* **2002**, *45*, 855–863.
18. Choi, S. U. S. Nanofluids: From Vision to Reality through Research. *J. Heat Transfer* **2009**, *131*, 033106–9.
19. Song, L.; Ci, L.; Lu, H.; Sorokin, P. B.; Jin, C.; Ni, J.; Kvashnin, A. G.; Kvashnin, D. G.; Lou, J.; Yakobson, B. I.; Ajayan, P. M. Large Scale Growth and Characterization of Atomic Hexagonal Boron Nitride Layers. *Nano Lett.* **2010**, *10*, 3209–3215.
20. Huxtable, T.; Cahill, D. G.; Shenogin, S.; Xue, L.; Ozisik, R.; Barone, P.; Usrey, M.; Strano, M. S.; Siddons, G.; Shim, M.; Keblinski, P. Interfacial Heat Flow in Carbon Nanotube Suspensions. *Nat. Mater.* **2003**, *2*, 731–734.
21. Xie, H.; Chen, L. Review on the Preparation and Thermal Performances of Carbon Nanotube Contained Nanofluids. *J. Chem. Eng. Data* **2011**, *56*, 1031–1041.
22. Gupta, S. S.; Siva, V. M.; Krishanan, S.; Sreeprasad, T. S.; Singh, P. K.; Pradeep, T.; Das, S. K. Thermal Conductivity Enhancement of Nanofluids Containing Graphene Nanosheets. *J. Appl. Phys.* **2011**, *110*, 084302.
23. Baby, T. T.; Ramaprabhu, S. Investigation of Thermal and Electrical Conductivity of Graphene Based Nanofluids. *J. Appl. Phys.* **2010**, *108*, 124308.
24. Yu, W.; Xie, H.; Bao, D. Enhanced Thermal Conductivities of Nanofluids Containing Graphene Oxide Nano Sheets. *Nanotechnology* **2010**, *21*, 055705.
25. Larson, R. G. *The Structure and Rheology of Complex Fluids*; Oxford University Press: New York, 1999.
26. Botha S. S. Synthesis and Characterization of Nanofluids for Cooling Applications. Ph.D. Thesis, University of the Western Cape, 2007.
27. Hinch, E. J.; Leal, L. G. The Effect of Brownian Motion on the Rheological Properties of a Suspension of Non-spherical Particles. *J. Fluid Mech.* **1972**, *52*, 683–712.
28. Hong, H.; Wensel, J.; Peterson, S.; Roy, W. Efficiently Lowering the Freezing Point in Heat Transfer Coolants Using Carbon Nanotubes. *J. Thermophys. Heat Transfer* **2007**, *12*, 446–448.